

SIMULATED EXPOSURE OF TITANIUM DIOXIDE MEMRISTORS TO ION BEAMS

by

**Nada S. MARJANOVIĆ¹, Miloš Lj. VUJISIĆ^{1*}, Kovička Dj. STANKOVIĆ¹,
Dejan DESPOTOVIĆ², and Predrag V. OSMOKROVIĆ¹**

¹Faculty of Electrical Engineering, University of Belgrade, Belgrade, Serbia
²Informatika AD, Belgrade, Serbia

Scientific paper

UDC: 621.382.2/.3:519.245:539.12-17

DOI: 10.2298/NTRP1002120M

The effects of exposing titanium dioxide memristors to ion beams are investigated through Monte Carlo simulation of particle transport. A model assuming ohmic electronic conduction and linear ionic drift in the memristor is utilized. The memristor is composed of a double-layer titanium dioxide thin film between two platinum electrodes. Obtained results suggest that a significant generation of oxygen ion/oxygen vacancy pairs in the oxide is to be expected along ion tracks. These can influence the device's operation by lowering the resistance of the stoichiometric oxide region and the mobility of the vacancies. Changes induced by ion irradiation affect the current-voltage characteristic and state retention ability of the memristor. If the displaced oxygen ions reach the platinum electrodes, they can form the O₂ gas and cause a permanent disruption of memristor functionality.

Key words: memristor, titanium dioxide, ion beam, Monte Carlo simulation

INTRODUCTION

In 2008, a two-terminal physical realization of a memristor was constructed by the HP Labs, a device that had been theoretically anticipated 37 years before [1, 2]. The constructed memristor is composed of a titanium dioxide thin film between two platinum electrodes. The oxide layer further consists of an insulating TiO₂ layer and a conducting oxygen-deficient TiO_{2-x} layer. Oxygen vacancies in the TiO_{2-x} layer act as mobile positively charged dopants which can drift in the electric field created by a voltage applied to the device's terminals. The total resistance of the device is determined as a series connection of the highly resistive stoichiometric layer and the conducting oxygen-poor layer. When a voltage is applied, the oxygen vacancies drift, shifting the boundary between the high-resistance and low-resistance layers. Total resistance is, thus, dependent on the charge which has passed through the memristor. Additionally, if the applied voltage is removed, the memristor "remembers" its last state, *i. e.* the value of total resistance at the moment of voltage suspension [1].

Ohm's law relation between voltage and current is

$$v(t) = R_{\text{ON}} \frac{w(t)}{D} + R_{\text{OFF}} \left(1 - \frac{w(t)}{D}\right) i(t) \quad (1)$$

where $w(t)$ is the size of the oxygen-poor layer, while R_{ON} and R_{OFF} are the resistances of the oxygen-deficient and the stoichiometric region, respectively, given for the full length D of the device. Relating $w(t)$ to the electronic charge that has passed through the device, the current-voltage (i - v) characteristic of the memristor is derived as [3]

$$i(t) = \frac{v(t)}{R_0 \sqrt{1 \mp 2\Delta R \frac{\mu_{\text{OV}} R_{\text{ON}}}{D^2 R_0^2} \int_0^t v(\tau) d\tau}} \quad (2)$$

where μ_{OV} is the mobility of oxygen vacancies in titanium dioxide, $R_0 = R_{\text{ON}}(w_0/D) + R_{\text{OFF}}(1 - w_0/D)$ is the effective resistance at $t = 0$, and $\Delta R = R_{\text{OFF}} - R_{\text{ON}}$. The minus sign in the denominator of eq. (2) applies when the oxygen-poor region is expanding, while the plus sign corresponds to the shrinking of this region. Since the mobility of oxygen vacancies in titanium dioxide is low ($\mu_{\text{OV}} \sim 10^{-10}$ cm²/Vs [4]), memristive effects are observed only when the memristor size D is nano-scale.

A typical memristor i - v curve for a sinusoidal driving voltage, obtained theoretically from eq. (2) as

* Corresponding author; e-mail: vujisa@ikomline.net

a 2-D parametric plot, is shown in fig. 1. It has the form of a double-loop hysteresis, with segments of negative differential resistance corresponding to the intervals during which w is increasing while $v(t)$ is already in recess, but still of same polarity. A similar hysteresis is obtained for any symmetrical AC voltage applied to the memristor. The hysteresis is observed only for small-amplitude (~ 1 V) voltages at frequencies below several kHz, for which w never reaches either of the limiting values (0 or D), *i. e.* the low-resistance oxygen-poor layer never stretches across the length of the device, nor does it vanish completely. For high-frequency low-amplitude AC voltages, the size of the oxygen-deficient layer barely changes for the duration of the voltage half-period, making the effective resistance of the memristor nearly constant and reducing the i - v hysteresis to a straight line, which is also presented in fig. 1.

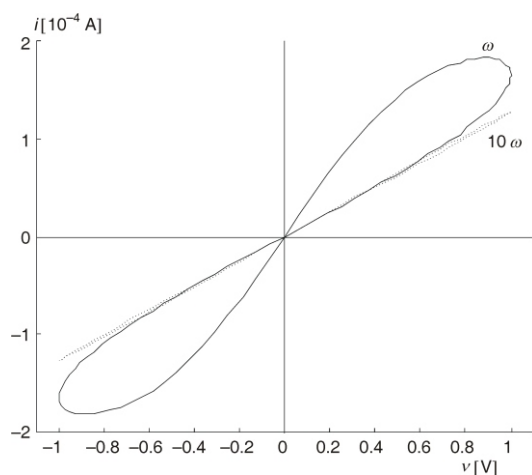


Figure 1. Current-voltage characteristic of the titanium dioxide memristor with ohmic electronic conduction and linear ionic drift of oxygen vacancies. The applied voltage is $v(t) = v_0 \sin(\omega t)$, with $v_0 = 1$ V and $\omega = \pi/10$ s $^{-1}$. Other parameters are: $R_{ON} = 100$ Ω , $R_{OFF} = 16$ k Ω , $D = 60$ nm, $w_0 = 30$ nm, $\mu_{OV} = 10^{-10}$ cm 2 /Vs. The dotted plot is for a ten-time higher frequency of the sinusoidal voltage

The value of w can be pushed to one of the limits either by large applied voltages or by long times under same polarity bias. Boundary states differ greatly in resistance, forming the basis of memristor bipolar switching. If the voltage across memristor terminals is suddenly suspended, the value of memristance is frozen and stays unchanged while there is no bias.

Memristor resistance is dependent on the distribution of oxygen vacancies, and it is therefore to be expected that the operation of this device is sensitive to ion bombardment which could cause displacements of additional oxygen atoms and thus perturb the distribution of vacancies. This paper examines the influence of ion beam exposure on the shape of the TiO₂

memristor's i - v hysteresis and on state retention when the memristor is used as a switch.

RESULTS OF ION TRANSPORT SIMULATIONS

Monte Carlo simulations of ion beams traversing the Pt-TiO₂-TiO_{2-x}-Pt memristor structure were performed in the TRIM part of the SRIM software package [5-7]. The default values of threshold displacement energy for oxygen and titanium atoms in the titanium dioxide provided by SRIM were changed to values obtained by a molecular dynamics simulation study for the rutile phase of TiO₂ (65 eV for oxygen and 130 eV for titanium) [8]. Instead of a calculated value for the density of TiO_{1.95} offered by SRIM, a more realistic value of 4.097 g/cm³ reported in [9] was used. The dimensions of the memristor structure are based on the values reported in [10].

The simulations were run with monoenergetic unidirectional ion beams, incident perpendicularly on the sides of the stack of materials constituting the memristor. Beam energy was varied for different ion species, commonly encountered in standard doping and implantation processes. All simulations were performed for the memristor state corresponding to $w = D/2$.

The number of atomic displacements is in direct proportion to the fluence of an incident ion beam, *i. e.* to the number of ions followed in the Monte Carlo simulation. Results presented in figs. 2 through 5 are from simulation runs with lower counts of incident ions, so that the graphs of particle and ion tracks would not be indiscernible. Results for energies and directions of the beams that resulted in a substantial displacement of oxygen atoms in the stoichiometric oxide layer, in comparison to the concentration of oxygen vacancies in the oxygen-deficient layer, are presented selectively. The aim is to point out that parallel ion beams of certain energies would indeed cause massive production of oxygen ion/oxygen vacancy pairs in the TiO₂ region, even in oxides less than 50 nm thick.

Figure 2(a) shows the trajectories of fifty 5 keV boron ions traversing the memristor structure, along with the accompanying tracks of displaced O and Ti atoms. The incident proton beam is perpendicular to the surface of the left platinum electrode. The thicknesses of the layers along the horizontal axis are as follows: 3 nm platinum layer, 15 nm stoichiometric TiO₂ layer, 15 nm oxygen-deficient TiO_{2-x} layer ($x = 0.05$), and another 3 nm platinum layer. The total length of the titanium dioxide film is, then, $D = 30$ nm. Figure 2(b) shows the distribution of oxygen vacancies, produced both by boron ions and in the cascades of displaced O and Ti atoms. Figures 2(c) and 2(d) show the tracks and oxygen vacancy distribution, respectively, but for a 10 keV boron ion beam. For the lower beam energy

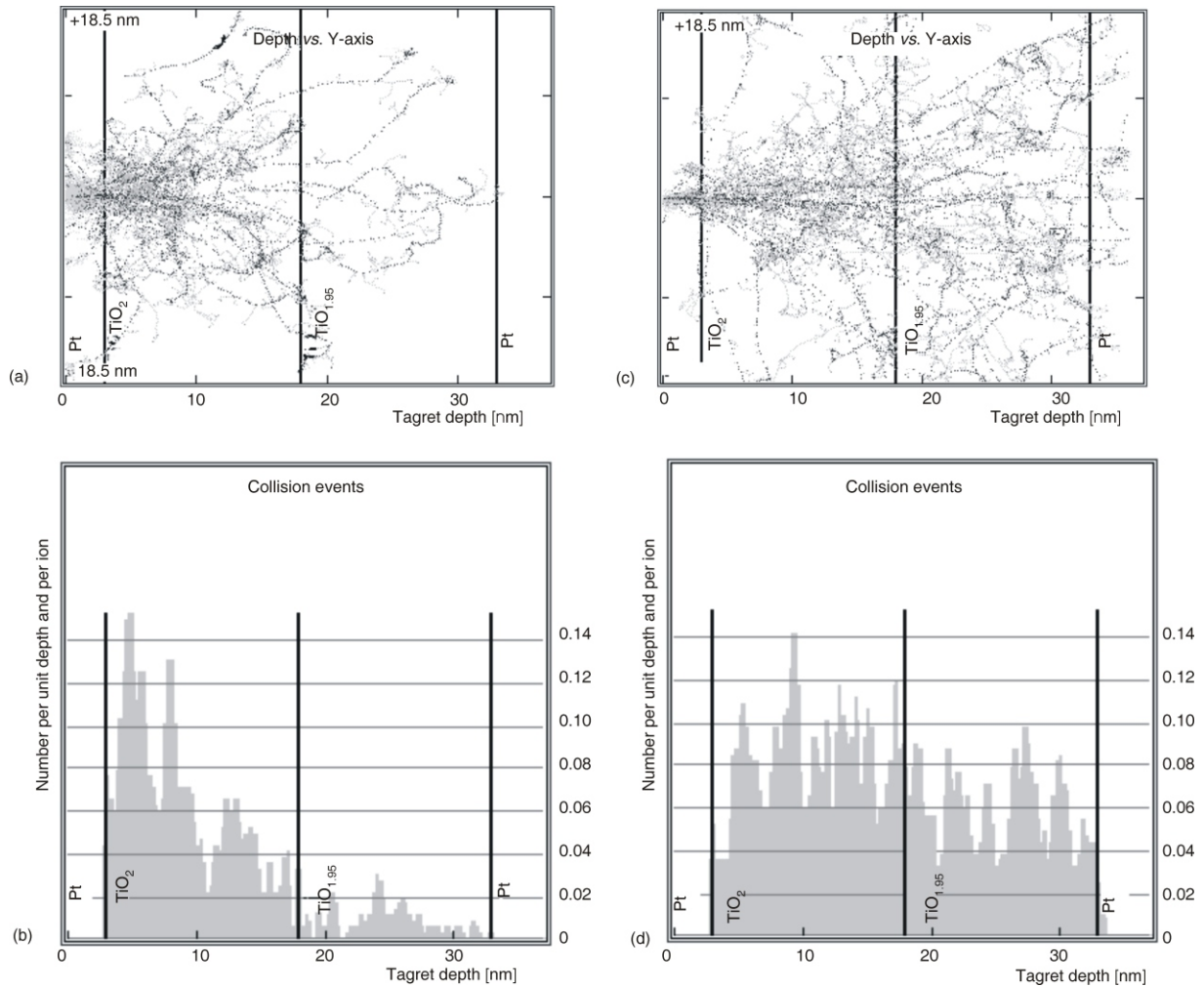


Figure 2. Simulation results for a beam of 50 boron ions incident perpendicularly on the left side of the Pt-TiO₂-TiO_{1.95}-Pt structure with a total thickness of 36 nm

(a) particle tracks for 5 keV boron ions; (b) Distribution of oxygen vacancies for the 5 keV boron ion beam; (c) Particle tracks for 10 keV boron ions; (d) distribution of oxygen vacancies for the 10 keV boron ion beam

(5 keV), ion tracks and oxygen vacancies are almost entirely contained within the stoichiometric TiO₂ layer, whereas for the higher energy (10 keV), they are spread more uniformly across the two oxide layers. The influence of the ion beam on the resistance of the stoichiometric region, and consequently on memristor operation, is more pronounced for lower energy boron ions.

Figure 3(a) shows the particle tracks when the memristor is exposed to ten 100 keV phosphorus ions, while fig. 3(b) presents the distribution of oxygen vacancies in this case. Substantial generation of oxygen vacancies in both oxide layers is again observed.

Distributions of Ti and O ions, displaced in direct interactions with the ions, or in subsequent cascade collisions when the memristor is exposed to one hundred 50 keV iron ions are shown in fig. 4(a). It is evident that the displacement of oxygen atoms is quite marked. Some oxygen ions may recombine with the vacancies,

but a large portion of the newly created vacancies remain, with the distribution shown in fig. 4(b).

Particle trajectories along the track of a single 50 keV arsenic ion incident perpendicularly on the left side of the Pt-TiO₂-TiO_{1.95}-Pt structure are shown in fig. 5. This figure illustrates the fact that even a single As ion traversing the memristor can create a considerable amount of oxygen vacancies in the stoichiometric TiO₂ layer.

ANALYSIS AND DISCUSSION

As Monte Carlo simulations of ion transport show, said radiations can generate a significant amount of oxygen ion/oxygen vacancy pairs in both high and low-resistance layers of titanium dioxide. A large number of titanium atom displacements also occur throughout the oxide. Primary displaced (knock-on) titanium

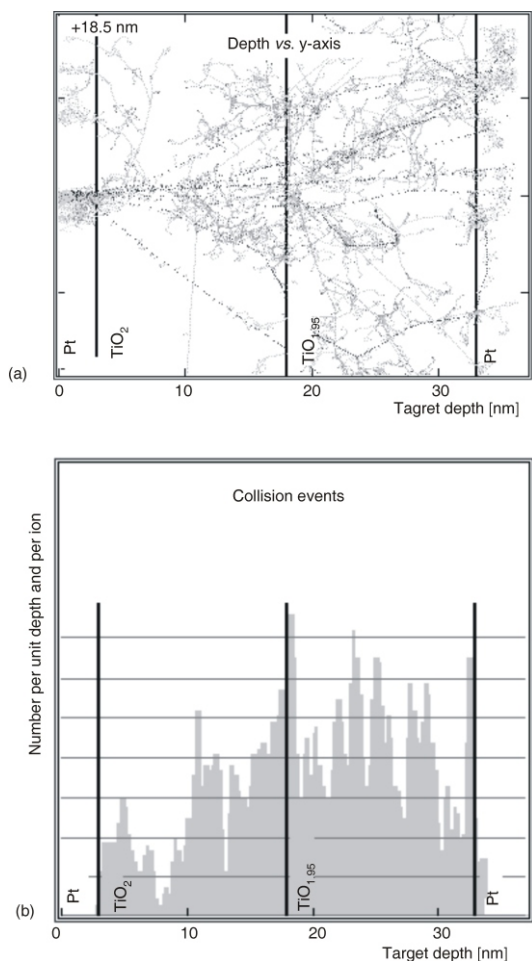


Figure 3. Simulation results for a beam of ten 100 keV phosphorus ions incident perpendicularly on the left side of the Pt-TiO₂-TiO_{1.95}-Pt structure with a total thickness of 36 nm

(a) Particle tracks; (b) Distribution of oxygen vacancies

and oxygen atoms cause further atomic displacements, producing a displacement tree.

Owing to its nano-size, the titanium dioxide memristor is immune to ions with energies >10 MeV. The non-ionizing energy loss of these high energy ions is significantly lower and they traverse the volume of the device along almost straight trajectories with proportionally less displacements. Whereas the electronic conductivity of the low-resistance oxygen-poor region is little affected by the appearance of additional vacancies, the effect on the conductance of the stoichiometric vacancy-free TiO₂ region can be considerable. Radiation-induced emergence of oxygen vacancies in the stoichiometric region can cause its resistance R_{OFF} to drop, disrupting the R_{OFF}/R_{ON} ratio of the memristor. The change of the resistance ratio affects the memristor $i-v$ characteristic through quantities R_0 and ΔR in eq. (2). The effect that the decrease of R_{OFF} has on the memristor $i-v$ curve is illustrated in fig. 6.

Titanium and oxygen ions produced by radiation in the stoichiometric layer can become interstitial at-

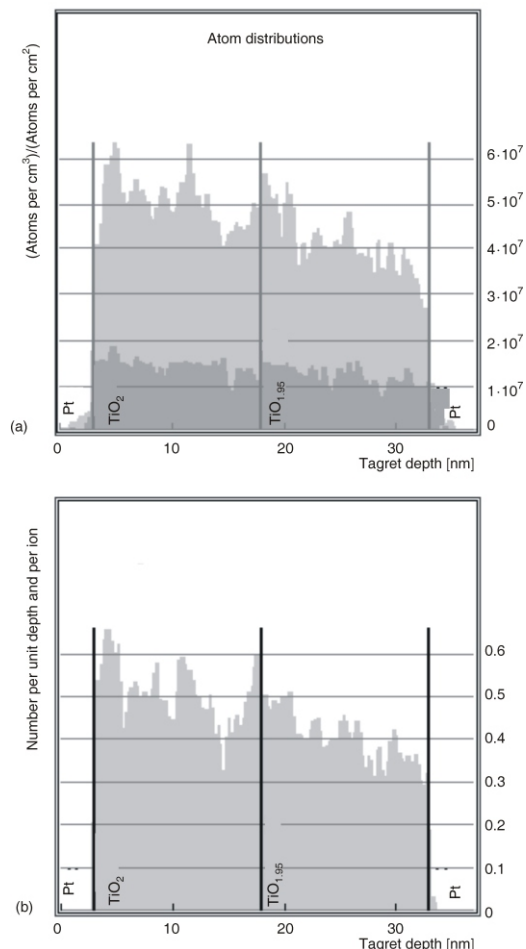


Figure 4. Simulation results for a beam of one hundred 50 keV iron ions incident perpendicularly on the left side of the Pt-TiO₂-TiO_{1.95}-Pt structure with a total thickness of 36 nm

(a) Distribution of displaced oxygen and titanium atoms; (b) Distribution of oxygen vacancies

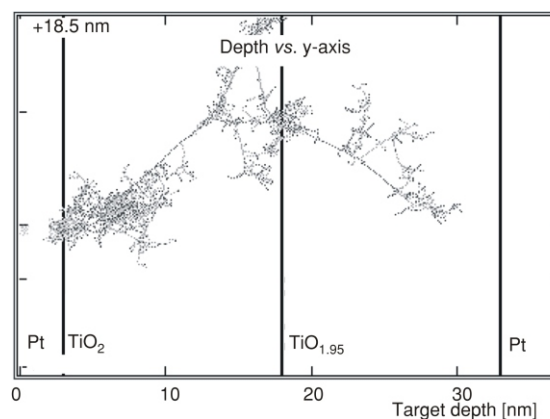


Figure 5. Particle tracks for a single 50 keV arsenic ion incident perpendicularly on the left side of the Pt-TiO₂-TiO_{1.95}-Pt structure

oms or migrate in the electric field. If the amplitude of the applied voltage is high enough, oxygen ions may

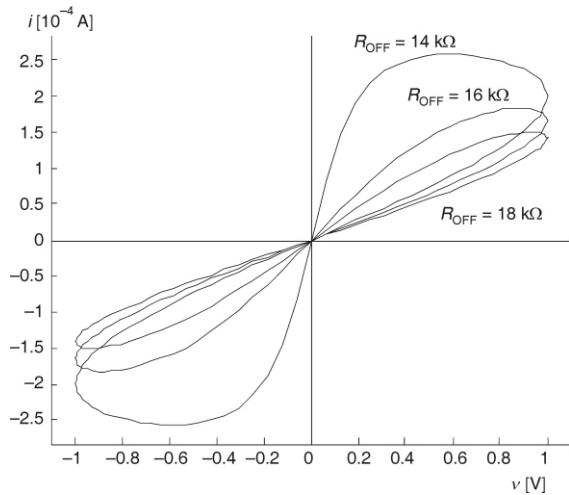


Figure 6. Current-voltage curves of a titanium dioxide memristor plotted for three different values of the stoichiometric region resistance: $R_{OFF} = 18 \text{ k}$, 16 k and 14 k

(The applied sinusoidal voltage and all other parameters are the same as for fig. 1)

reach one of the electrodes where they can form the O_2 gas and cause the deformation of the oxide/metal interface, leading to a permanent disruption of memristor operation [11, 12]. The presence of titanium and oxygen atoms can also reduce the mobility of oxygen vacancies μ_{OV} [13, 14]. According to eq. (2), a decrease of μ_{OV} affects the memristor $i-v$ hysteresis, as shown by example plots in fig. 7.

The specific switching functionality of a memristor rests on the high R_{OFF}/R_{ON} ratio which enables two boundary states to be unambiguously distinguishable by a read voltage signal, as well as on its

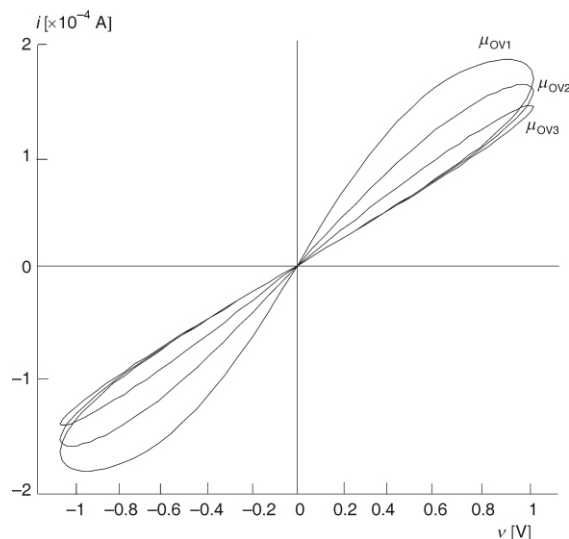


Figure 7. Current-voltage curves of a titanium dioxide memristor, plotted for three different values of oxygen vacancy mobility: $\mu_{OV1} = 10^{-10} \text{ cm}^2/\text{Vs}$, $\mu_{OV2} = 0.8 \cdot 10^{-10} \text{ cm}^2/\text{Vs}$, and $\mu_{OV3} = 0.5 \cdot 10^{-10} \text{ cm}^2/\text{Vs}$

(The applied sinusoidal voltage and all other parameters are the same as for fig. 1)

ability to hold a state at zero bias. Since for the highly conducting boundary state, corresponding to $w = D$, the low-resistance region stretches across the whole of the oxide, the radiation produced change of R_{OFF} has no effect on state retention. The high-total-resistance state is, however, susceptible to change when exposed to ion bombardment. This state, corresponding to $w = 0$, is characterized by a diminished or non-existent oxygen-poor region, with the total memristor resistance approximately equal to R_{OFF} . The decrease of R_{OFF} caused by irradiation can therefore perturb this state, resulting in an error at readout [15, 16].

CONCLUSIONS

Exposure of a titanium dioxide memristor to beams of ions can influence the device's operation in several ways. A significant generation of oxygen ion/oxygen vacancy pairs in the oxide is to be expected, as suggested by Monte Carlo simulations of ion transport. Radiation induced appearance of oxygen vacancies in the stoichiometric TiO_2 layer can cause its resistance to drop, producing a counter-clockwise rotation of the memristor $i-v$ curve and a larger swing in its double-loops. The presence of titanium and oxygen ions and interstitial atoms, displaced by the radiation, can reduce the mobility of oxygen vacancies, causing the memristor $i-v$ curve to rotate clockwise. When the memristor is operated as a switching element of a non-volatile memory, e. g. within a crossbar array, the high-total-resistance state, characterized by a diminished oxygen-poor region, can be perturbed by irradiation and result in an erroneous readout. Finally, if the displaced oxygen ions reach the platinum electrodes, they can form the O_2 gas and cause a permanent disruption of memristor functionality.

ACKNOWLEDGEMENT

This work was supported by the Ministry of Science and Environmental Protection of the Republic of Serbia under contract 141046.

REFERENCES

- [1] Strukov, D. B., Snider, G. S., Stewart, D. R., Williams R. S., The Missing Memristor Found, *Nature*, 453 (2008), pp. 80-83, doi: 10.1038/nature06932
- [2] Chua, L. O., Memristor – the Missing Circuit Element, *IEEE Trans. Circuit Theory*, 18 (1971), 5, pp. 507-519
- [3] Joglekar, Y. N., Wolf, S. J., The Elusive Memristor: Properties of Basic Electrical Circuits, *Eur. J. Phys.*, 30 (2009), 4, pp. 661-675
- [4] Zhang, Z., Ge, Q., Li, S., Kay, B. D., White, J. M., Dohnálek, Z., Imaging Intrinsic Diffusion of

- Bridge-Bonded Oxygen Vacancies on TiO₂(110), *Phys. Rev. Lett.*, 99 (2007), paper no. 126105
- [5] Ziegler, J. F., Biersack, J. P., Ziegler, M. D., SRIM (The Stopping and Range of Ions in Matter), available online: <http://www.srim.org>
- [6] Osmokrović, P., Jurosević, M., Stanković, K., Vujisić, M., Radiation Hardness of Gas Discharge Tubes and Avalanche Diodes used for Transient Voltage Suppression, *Radiation Effects and Defects in Solids*, 164 (2009), 12, pp. 800-808
- [7] Stanković, K., Vujisić, M., Dolićanin, E., Reliability of Semiconductor and Gas-Filled Diodes for Over-Voltage Protection Exposed to Ionizing Radiation, *Nuclear Technology & Radiation Protection*, 24 (2009), 2, pp. 132-137
- [8] Thomas, B. S., Marks, N. A., Corrales, L. R., Devanathan, R., Threshold Displacement Energies in Rutile TiO₂: A Molecular Dynamics Simulation Study, *Nucl. Instr. and Meth. B*, 239 (2005), 3, pp. 191-201
- [9] Minnear, W. P., Bradt, R. C., Stoichiometry Effects on the Fracture of TiO_{2-x}, *Journal of the American Ceramic Society*, 63 (1980), pp. 485-489
- [10] Williams, R. S., How We Found The Missing Memristor, *IEEE Spectrum*, 45 (2008), 12, pp. 28-35
- [11] Yang, J. J., Pickett, M. D., Li, X., Ohlberg, D. A. A., Stewart, D. R., Williams, R. S., Memristive Switching Mechanism for Metal/Oxide/Metal Nanodevices, *Nat. Nanotechnol.*, 3 (2008), 7, pp. 429-433
- [12] Stanković, K., Vujisić, M., Influence of Radiation Energy and Angle of Incidence on the Uncertainty in Measurements by GM Counters, *Nuclear Technology & Radiation Protection*, 23 (2008), 1, pp. 41-42
- [13] ***, Physics of Solid State Ionics (Eds. T. Sakuma, H. Takahashi), Research Signpost, Kerala, India, 2006
- [14] Vujisić, M., Stanković, K., Dolićanin, E., Jovanović, B., Radiation Effects in Polycarbonate Capacitors, *Nuclear Technology & Radiation Protection*, 24 (2009), 2, pp. 209-211
- [15] Vujisić, M., Stanković, K., Vasić, A., Comparison of Gamma Ray Effects on EPROMs and E²PROMs, *Nuclear Technology & Radiation Protection*, 24 (2009), 1, pp. 61-67
- [16] Vujisić, M., Stanković, K., Dolićanin, E., Osmokrović, P., Radiation Hardness of COTS EPROMs and E²PROMs, *Radiation Effects and Defects in Solids*, 165 (2010), 5, pp. 362-369

Received on May 4, 2010
Accepted on June 28, 2010

**Нада С. МАРЈАНОВИЋ, Милош Љ. ВУЈИСИЋ, Ковиљка Ђ. СТАНКОВИЋ,
Дејан ДЕСПОТОВИЋ, Предраг В. ОСМОКРОВИЋ**

**СИМУЛАЦИЈА ИЗЛАГАЊА МЕМРИСТОРА ОД
ТИТАНИЈУМ-ДИОКСИДА ЈОНСКИМ СНОПОВИМА**

У раду се изучавају ефекти излагања мемристора на бази титанијум-диоксида дејству јонских снопова, применом Монте Карло симулације транспорта честица. Коришћен је модел мемристора који претпоставља омску електронску проводност и линеаран дрифт јона. Мемристор се састоји од двослојног танког филма титанијум-диоксида који се налази између двеју електрода од платине. Добијени резултати указују да дуж трајекторија јона у оксиду долази до значајног генерисања парова које сачињавају јон кисеоника и кисеонична ваканција. Ови парови могу да утичу на рад компоненте путем смањења отпорности стоихиометријског слоја у оксиду и покретљивости кисеоничних ваканција. Промене изазване излагањем јонском снопу утичу на струјно-напонску карактеристику мемристора, као и на способност задржавања запамћеног стања. У случају да измештени јони кисеоника доспеју до електрода од платине, могуће је образовање O₂ гаса, што трајно нарушава функционалност мемристора.

Кључне речи: мемристор, титанијум-диоксид, јонски сноп, Монте Карло симулација